

12/10/90
M.L.P.

①

PONF. 9009123-60

SLAC-PUB--5333

DE91 004688

(A)

PERFORMANCE OF THE 2 MeV MICROWAVE GUN FOR THE SSRL 150 MeV LINAC*

M. Borland,¹ M. C. Green,² R. H. Miller,³ L. V. Nelson,² E. Tanabe,^{3,4} J. N. Weaver,¹ and H. Wiedemann¹

¹ AET Associates, Cupertino, CA 95014

² Stanford Synchrotron Radiation Laboratory, Stanford University, Stanford, CA 94309

³ Stanford Linear Accelerator Center, Stanford University, Stanford, CA 94309

⁴ Varian Associates, Palo Alto, CA 94303

Abstract

As described in a previous article,¹ the pre-injector linac for SSRL's 3 GeV synchrotron is fed by a 2 MeV, 1.5 A, low-emittance microwave gun, consisting of a thermionic cathode mounted in the first cell of a 1-1/2-cell S-band cavity. In this article, we report on the successful operation of the low-emittance gun, the longitudinally-bunching alpha-magnet, and the three-microbunch FET-pulsed beam-chopper. Simulations predict a normalized rms emittance at the gun exit of less than $10 \pi \cdot m_e c \cdot \mu\text{m}$; chromatic effects in transport optics increase this to approximately $30 \pi \cdot m_e c \cdot \mu\text{m}$. The gun was specifically designed to have a longitudinal phase-space suited to magnetic compression, as a result of which we predict that peak currents in excess of 300 A in a 1 ps bunch are feasible with the existing alpha-magnet. Results of simulations and experiments will be presented and compared.

Introduction

A variety of applications demand low-emittance, high-current electron beams. Among these are free-electron lasers, linear colliders, novel acceleration methods, and synchrotron radiation from micro-undulators. A number of approaches are discussed in the literature^{2,3,4} that address the problem of producing low-emittance, high-current beams. Among these are very small cathodes, laser-pulsed photocathodes, RF fields in the gun, multistage bunching, subharmonics in the accelerating field, and damping rings.

Each of these ideas is an attempt to deal with one or more of the effects that can spoil beam-emittance as current is increased. Among these effects are space-charge forces, time-dependent focusing from RF fields, nonlinear transverse RF fields, and beam-transport aberrations. The microwave-gun concept⁵ attempts to obtain lower emittance by rapidly accelerating the electron beam, using the high gradients possible in an RF cavity. Several successful microwave gun designs exist that utilize photocathodes,^{6,7} and these show the greatest promise as "solutions" to the problem of low emittance and high current. However, the addition of the laser and photocathode greatly increases the complexity and cost of the gun, so that for many applications

a thermionic microwave gun is more appropriate. Compared to conventional DC gun systems, a thermionic microwave gun can provide several orders of magnitude increase in peak current and brightness, without a significant increase in system complexity.

Gun Design Overview

The SSRL RF gun was designed in collaboration by SSRL, AET Associates, and Varian Associates, for use as the electron source for the SSRL 150 MeV linear accelerator, as part of the SSRL 3 GeV Injector Project. While the needs of the Injector Project did not demand a gun with the performance level of the SSRL RF gun, it did provide an opportunity for research that a system based on a DC gun would not have provided.

The gun design had a number of goals, which were chosen not only with the needs of the SSRL Injector in mind, but also with the intention of producing an electron source appropriate for some of the applications mentioned above. These goals were:

1. For a current density at the cathode of $J \leq 100 \text{ A/cm}^2$, each bunch injected into the linac should contain at least 10^9 usable electrons; i.e., electrons with momenta $\geq 80\%$ of the peak momentum in the bunch.
2. Peak momentum of 2 to 3 MeV/c in the bunches, for peak on-axis electric fields in the second cell of less than 120 MV/m.
3. Near-linear, monotonic dependence of momentum $p(t)$ on exit-time for 20 to 40 ps during a bunch, in order to allow magnetic bunch compression.
4. Gently converging beam in the gun for a wide range of current densities ($J < 100 \text{ A/cm}^2$) for field levels that produce 2 to 3 MeV/c peak momentum.
5. Normalized rms emittance, $\epsilon_x \equiv \pi (\langle x^2 \rangle \langle p_x^2 \rangle - \langle x \cdot p_x \rangle^2)^{1/2}$, for the useful beam (as defined in goal 1) of less than $15 \pi \cdot m_e c \cdot \mu\text{m}$, over the same range of conditions.
6. Manageable (i.e., less than 5 W average at 10 pps for a 2 μs pulse) back-bombardment power due to electrons returning to hit the cathode.

*Work supported by Department of Energy contract DE-AC03-76SF00511.

Presented at the Linear Accelerator Conference, Albuquerque, New Mexico, September 10-14, 1990.

MASTER
DISTRIBUTION OF THIS DOCUMENT IS UNLIMITED

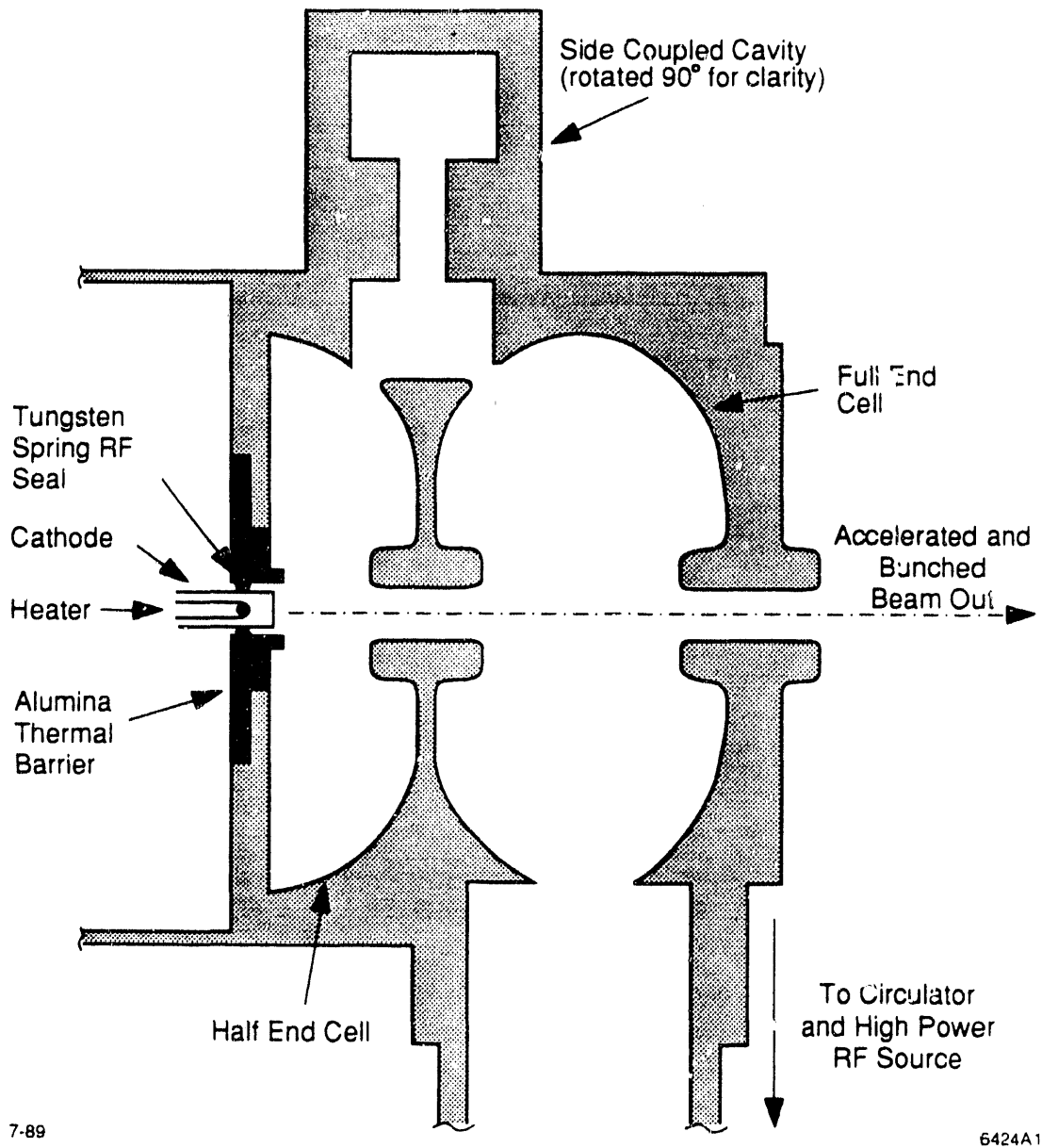


Fig. 1. Cross section of the gun cavity.

Figure 1 shows a cross-sectional view of the gun, which consists of a demountable, thermionic cathode in the first half-cell of a 1-1/2-cell S-band RF cavity. In order to thermally isolate the cathode from the metal walls of the cavity, the annular focusing structure around the cathode is also a thermal barrier made from metallized ceramic. RF electrical contact between the focusing structure and the cathode is obtained using a toroidal tungsten-wire spring around the cathode stem. Optical pyrometry shows that this configuration allows cathode temperatures of more than 1100°C to be obtained, with a temperature variation of less than 5°C over the cathode surface, which is 6 mm in diameter.

The assumptions of design goal 1 turned out to be conservative in terms of the current density needed to obtain the desired beam intensity. The limiting factor on current was, in fact, the amount of RF power available to the gun. Obtaining beam momenta of the level desired implies cavity wall losses of about 1 MW. It was anticipated that about 4 MW total RF power would be available to the gun, implying that 3 MW could go into the beam. For an average kinetic energy of 2 MeV, this implies that 1.5 A (3.3×10^9 electrons per bunch) could be accelerated, requiring $J \approx 30$ A/cm². In order to obtain a match to the RF source under these conditions, the normalized load impedance of the cavity without beam was chosen to be $\beta = 1 + P_{\text{beam}}/P_{\text{cavity}} \approx 4$.

In order to satisfy goals 2 and 3, it was necessary to alter the excitation ratio of the two cells from the usual one-to-one ratio. In particular, the excitation level of the second, full cell is approximately 2.9 times that of the first, half cell as seen in Fig. 2. This permits the gun to be operated over a wide range of gradient levels without obtaining the sinusoidal $p(t)$ curve that appears when particles arrive in the second cell ahead of the RF crest. If one characterizes the excitation level of the gun in terms of the peak, on-axis electric field at the RF crest in the second cell, E_{p2} , then operation in the range $50 \text{ MV/m} < E_{p2} < 90 \text{ MV/m}$ (giving maximum momentum between 1.3 MeV/c and 3.3 MeV/c) produces a beam that is compatible with magnetic compression. Higher excitation levels are preferred in order to obtain more efficient extraction of beam from the gun, resulting in higher currents for the same current density.

The shape of the focusing structure was arrived at using the PIC-code MASK⁸ in order to satisfy design goals 4 and 5. The shape of the cavities themselves was not altered appreciably from that used for Varian medical linacs. More details of the simulations were reported in an earlier article,¹ and further details will be made available in the future.⁹

As for design goal 6, it was found that back-bombardment power would exceed 5 W average cathode for current densities greater than about 50 A/cm² for the nominal operating gradient of $E_{p2} = 75$ MV/m. Fortunately, it is not necessary to use such high current densities in order to obtain the desired beam current (nor would it have been possible, given the available RF power).

Operating experience with the gun to date indicates that the design goals have been largely met. Specifics of the longitudinal and transverse phase space characterization are presented below. Here we offer a few general comments on our operating experience. Stable currents of up to 1.65 A (about 3.6×10^9 electrons per bunch) have been obtained with approximately 3.5 MW RF power, though the current installation of the gun does not provide sufficient RF power to exceed about 900 mA. While back-bombardment is in evidence, it is a relatively minor effect, permitting effective control of gun current via cathode filament power. The cathode currently in the gun (installed after the first cathode was poisoned by a vacuum leak) has been run for about 500 hours so far with no sign of degradation.

Gun-to-Linac Transport Line

The Gun-to-Linac transport line ("GTL line") shown schematically in Fig. 3 serves four main functions. Each of these functions will be mentioned briefly here, then discussed in more detail in subsequent sections.

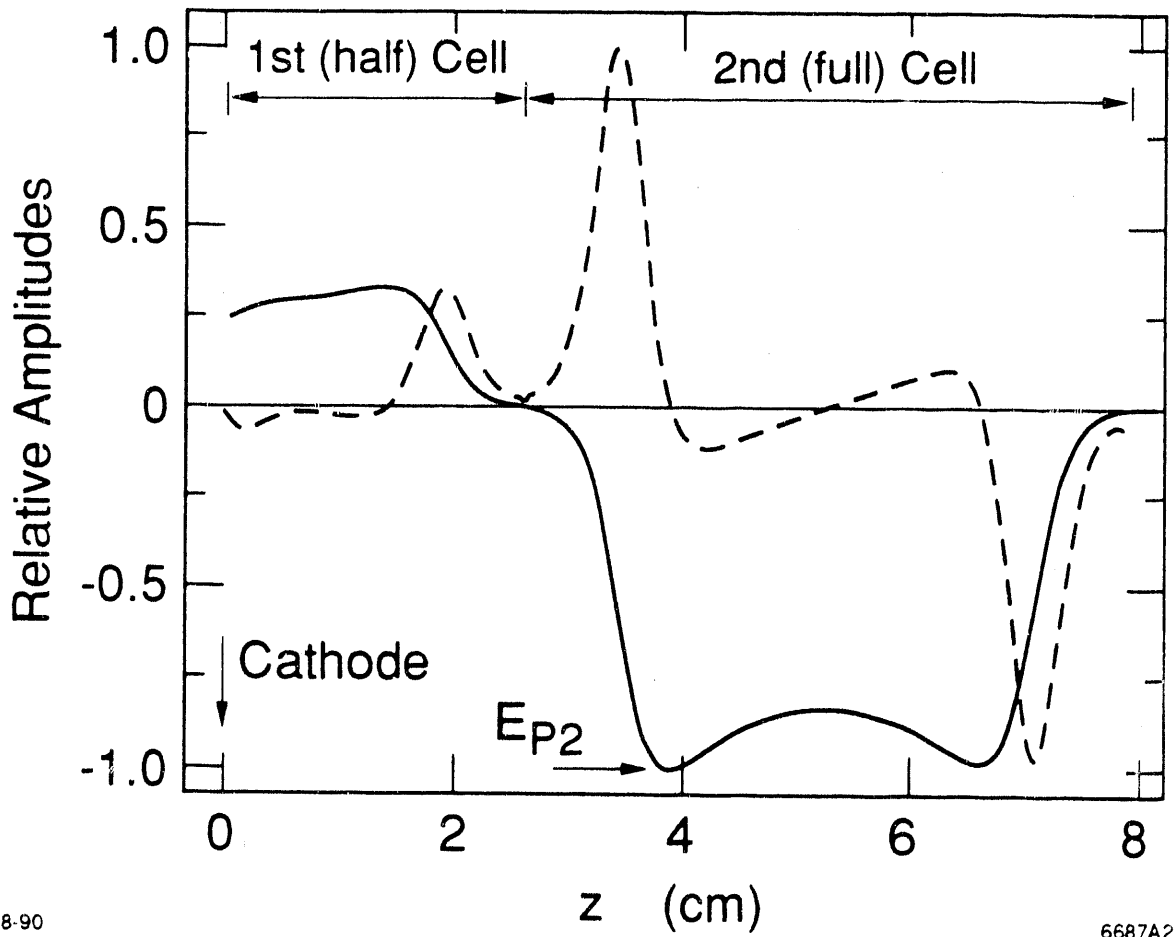
First, the GTL line provides bunching of the beam in order to match to the longitudinal acceptance of the linear accelerator, so that a small momentum spread is obtained at the end of the three accelerator sections.

Second, it allows the filtering out of low-momentum particles. These two functions are achieved using an alpha-magnet.¹⁰

Third, the GTL line contains quadrupoles and steering dipoles to control the transverse beam size and trajectory. Aside from the obvious need for such elements in order to obtain good transmission, the quadrupoles are required as part of the momentum filter (for good resolution), and to match the beam to the transverse acceptance of the accelerator, while at the same time providing a well-focused beam for proper operation of the chopper.

Fourth, the GTL line contains the FET-pulsed beam-chopper, permitting the injection into the linac of only three S-band bunches of the train of several thousand that emerge from the gun during the RF pulse; the rationale for this mode of operation will be discussed below.

Simulations of the GTL line are done using the second-order tracking/integrating code *elegant*⁹, which interfaces to MASK and allows a variety of numerical experiments (e.g., spectrum and emittance measurements) to be done with only modest effort. The code does not include space-charge effects, which is believed to be an acceptable approximation for the energy and current we are dealing with. Quadrupoles are simulated with fringe-fields using a trapezoidal approximation to the measured gradient as a function of longitudinal position. Alpha-magnets are implemented in terms of matrices, to third order.⁹



8-90

6687A2

Fig. 2. Radial (dashed) and longitudinal (solid) electric field profiles for the RF gun.

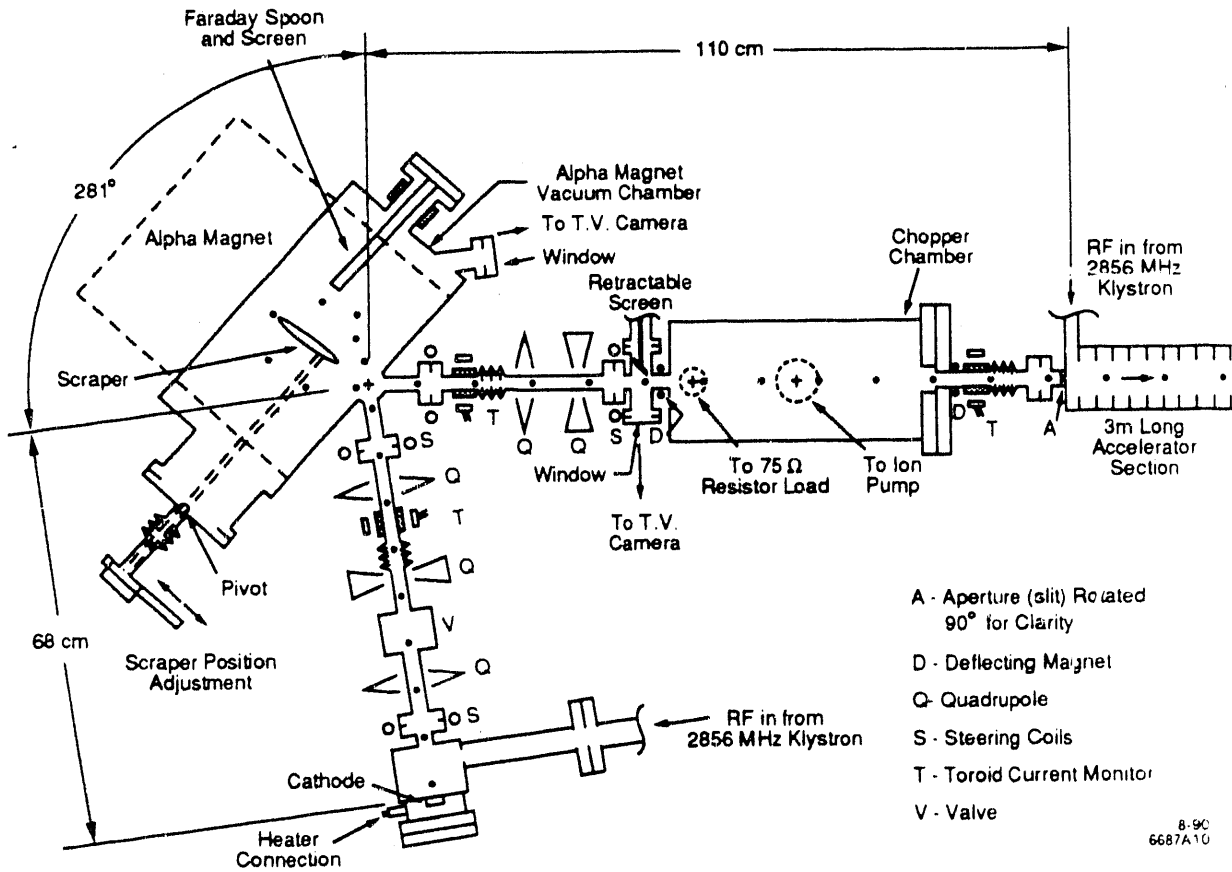


Fig. 3. Gun-to-linac layout.

Magnetic Bunch Compression

The principle of magnetic bunching can be used on a beamline with momentum-dependent path lengths, which in terms of the transport matrix of the beamline,¹¹ means a nonzero matrix element $R_{56} = \int [D(s)/\rho(s)] ds$, where D is the dispersion and ρ is the bending radius. An additional requirement for the beamline is zero dispersion at the end of the beamline, in order to avoid increasing the beam-size due to energy spread. Finally, in order to permit momentum filtration, it is necessary to have nonzero dispersion in a location where an obstruction can be moved into the beam. All of these requirements can be satisfied with a system containing an alpha magnet,¹⁰ which to first-order is achromatic in the transverse planes and has momentum-dependent path lengths.

The beam from the gun has a near-linear, monotonic dependence of exit time on momentum: $t_{\text{exit}}(p) \approx t_0 + (dt_{\text{exit}}/dp)_0 (p - p_0)$, where $(dt_{\text{exit}}/dp) < 0$ and $p \equiv \beta\gamma$. To bunch the beam, all particles of interest must arrive at the linac (or some distance inside it) at the same time; i.e., that $t_{\text{arrival}}(p) = t_{\text{exit}}(p) + \Delta t_{\text{drift}}(p) + \Delta t_{\alpha}(p) = \text{constant}$.

The time-of-flight in a drift space is $\Delta t_{\text{drift}}(p) = (L_{\text{drift}}/\beta c)$, while the time-of-flight in the alpha magnet is:

$$\Delta t_{\alpha}(p) = \frac{K_{\alpha}}{\beta c} \left(\frac{p}{\nabla B_{\alpha}} \right)^{1/2} \quad (\text{MKS}) \quad ,$$

where

$$K_{\alpha} = 4.64210 \left(\frac{m_e c}{e} \right)^{1/2} \quad (\text{MKS}) \quad ,$$

and the numerical constant, 4.64210, was determined by numerical integration.⁹ For reasonably small momentum spread, one can expand $t_{\text{arrival}}(p)$ to first order in $\delta = (p - p_0)/p_0$. Setting the term proportional to δ equal to zero, one obtains the condition for bunching:

$$\nabla B_{\alpha} = \frac{p_0 K_{\alpha}^2 [\beta_0 - 1/(2\beta_0)]^2}{\{c p_0 (dt_{\text{exit}}/dp) + L_{\text{drift}} [\beta_0 - 1/\beta_0]\}^2} \quad .$$

Beam Chopper

Since the SSRL gun uses a thermionic cathode, emission occurs throughout the RF pulse, resulting in the acceleration of several thousand S-band bunches out of the gun. Because of the intensity of these bunches, beam-loading in the subsequent linear accelerator sections would make it impossible to accelerate all of these bunches to the desired energy of 150 MeV. In addition, the booster RF frequency is 358 MHz, meaning that only three to five consecutive S-band bunches can be captured in a booster RF bucket. Hence, even if all of the bunches generated by the gun could be accelerated to the desired energy, at most 60% of the charge would be captured, implying high radiation levels due to the loss of the other 40% at 150 MeV.

Several solutions are possible. One is to have a resonant chopper (i.e., a transverse deflecting RF cavity) that would admit a train of "S-band triplets" into the linac at some subharmonic frequency of 358 MHz. While this would solve the problem with bunches being injected into the Booster at the wrong phase, it would still result in beam going into the Booster for a much longer time than necessary to fill the available Booster RF buckets. Hence, an additional chopper would be needed to limit the length of the train of triplets to permit filling of less than a third of the Booster circumference, consistent with the length of the injection and ejection kicker pulses. Even with such a system, the intensity of the individual bunches would be such as to produce significant beam-loading in the linear accelerator, meaning that the intensity of the individual bunches might need to be reduced in order to avoid excessive energy spread at injection.

A simpler solution is to attempt to inject a single S-band triplet into the linac, using a fast-pulsed transverse deflector capable of imparting significantly different deflection to bunches separately by only 350 ps. This is the system adopted, as shown schematically in Fig. 4. Before and after the chopper itself are permanent-magnet deflectors that serve to deflect the beam into an absorber when the chopper is off, and correct the angle of the bunches that emerge from the chopper when it is pulsed.

The chopper chamber contains a 0.4-m-long parallel-plate transmission line with a gap of 1.84 cm, down which is sent a pulsed (1.7 μs) TEM-mode wave that rises from 0 to 7 kV in 10 ns. Hence, during the pulser rise-time, bunches of momentum p separated in time by ΔT_b , experience deflections that differ by approximately $[2(dV/dt) \Delta T_b (1/\text{gap}) L_{\text{plates}}]/(pc)$. For a 2.5 MeV/c beam and the pulse parameters just given, this comes out to about a 4 mrad deflection between successive S-band bunches. Taking the distance, L_s , from the midpoint of the plates to the slits as the moment arm, one can calculate the approximate transverse displacement of subsequent bunches. In our case, $L_s = 0.33\text{m}$, giving a transverse displacement between bunches of just over 1 mm.

Using a slit with a full aperture of 4 mm and noting that the beam-size at the slits is ± 2 mm, this system will let through parts of seven bunches. Only for three of these bunches will most of the charge be let through. For two of the others, half of the charge will be let through, while the remaining two will have only a small amount of their charge admitted into the linac. Detailed simulations confirm that this rough calculation is valid, as does operational experience with the chopper.⁹ Images of the beam on a screen downstream of the chopper show three to five bunches separated vertically by the time-dependent deflection produced by the chopper.

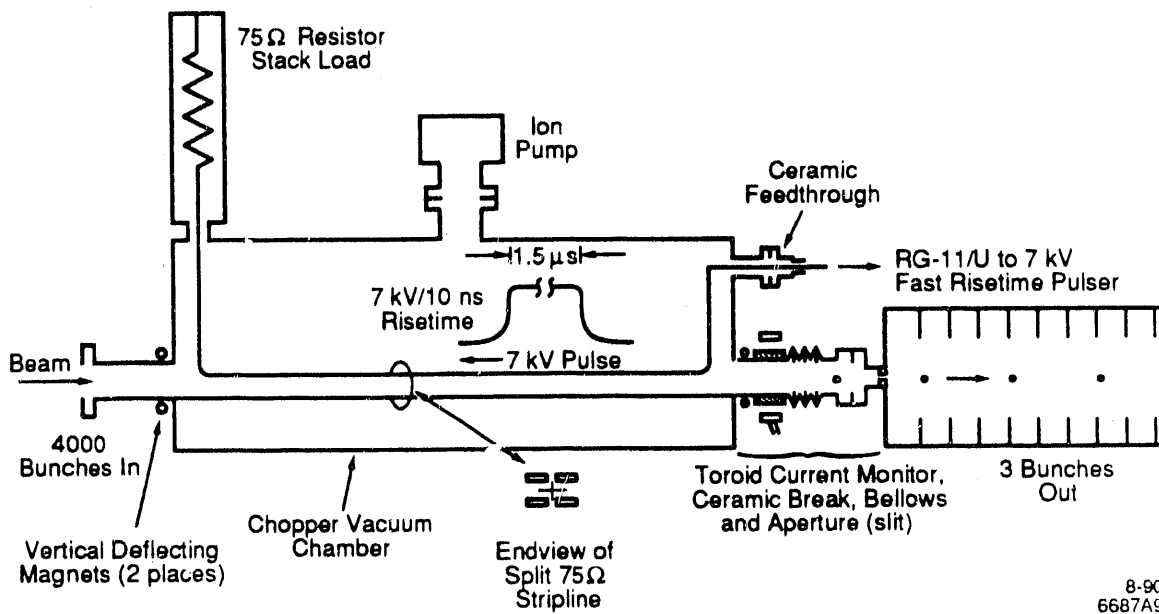
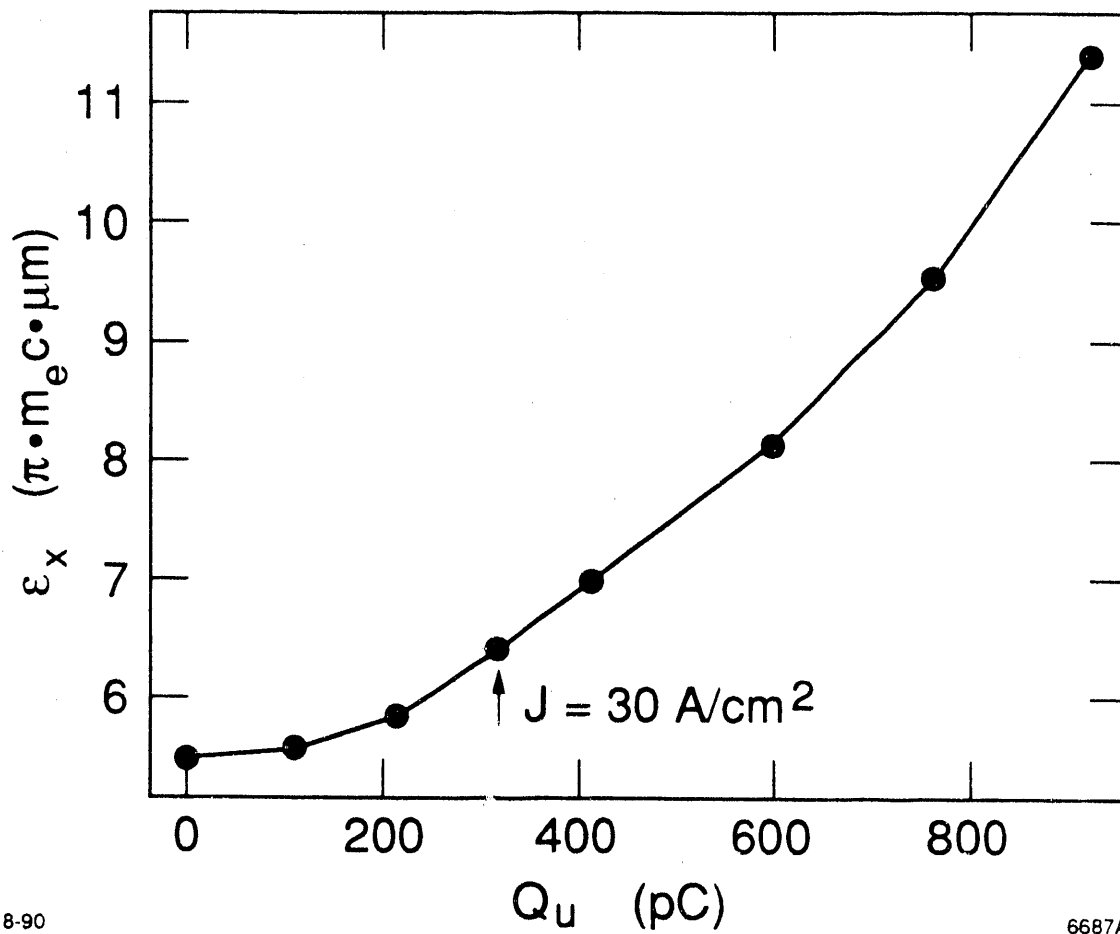


Fig. 4. Side view of the chopper.



8-90

6687A3

Fig. 5. Emittance versus charge per bunch.

Transverse Phase Space

Figure 5 shows the predicted, normalized rms emittance in each plane of the "useful" beam (as defined above) at the gun exit, as a function of charge in the beam obtained through variation of the current density in MASK simulations with $E_{p2} = 75$ MV/m. Note that the actual emittance at the end of the GTL line is predicted to be significantly greater than the emittance at the gun exit, because of chromatic aberrations in the quadrupoles and because we make use of $\pm 10\%$ momentum spread. In addition, because the alpha magnet introduces coupling, one can obtain significantly smaller emittance in one plane at the expense of larger emittance in the other plane. Because of these effects, it is better to speak in terms of the geometric mean, $\bar{\tau} = (\epsilon_x \epsilon_y)^{1/2}$ of the emittances in the two planes. Simulations predict that for our nominal operating gradient of $E_{p2} = 75$ MV/m, $\bar{\tau}$ at the end of the GTL is less than $30 \pi \cdot m_e c \cdot \mu\text{m}$ for current densities up to 40 A/cm², with only a weak dependence on current density, due in part to the overriding effect of chromatic aberrations (compare Fig. 5).

The GTL features an insertable screen just before the beam-chopper, which can be used in conjunction with the quadrupole just after the alpha magnet to make measurements of beam size versus quadrupole strength. This data can be used to deduce the sigma matrix, from which the emittance can be obtained.¹² Data from such a measurement at low current for the horizontal plane, together with results from a simulated measurement done using *elegant*, are shown in Fig. 6. The indicated normalized emittance from the experiment is approximately $35 \pi \cdot m_e c \cdot \mu\text{m}$, compared to $25 \pi \cdot m_e c \cdot \mu\text{m}$ from the simulation. Other measurements confirm horizontal normalized emittances in the range of 35 to $40 \pi \cdot m_e c \cdot \mu\text{m}$. As of this writing, measurements exist only for the horizontal plane. Future work will report on the emittances for both planes.

Longitudinal Phase-Space

Figure 7 shows MASK longitudinal phase-space results for the gun for typical running parameters of $E_{p2} = 75$ MV/m and $J = 10$ A/cm². As mentioned above, for a wide range of operating gradients, the longitudinal phase-space of the gun is characterized by a near-linear, monotonic dependence of momentum on exit-time. Note that the momentum distribution is well-peaked near the maximum momentum, and that the particles are similarly bunched in time. In general, about 50% of the particles exiting the gun are within 20% of the maximum momentum, and these same particles extend over about 25 ps. For higher currents at the same gradient, the momentum peak is broader, as expected from the mutual repulsion of electrons in the beam; roughly speaking, one might find as much as a factor of two broadening of the peak in going to

$J = 40$ A/cm² from $J = 10$ A/cm², depending on the gradient.

Spectrum measurements can be made using a moveable scraper in the alpha magnet, together with the current toroids before and after the alpha magnet. Given such measurements, one can make a number of comparisons with simulations. For example, one can look at the dependence of the position of the momentum peak on the gradient. Unfortunately, there are no field probes in the gun, so the gradient must be deduced from power conservation:

$$\begin{aligned} E_{p2} &\approx 69 (P_{\text{cavity}})^{1/2} \\ &= 69 (P_{\text{forward}} - P_{\text{reflected}} - P_{\text{beam}})^{1/2}, \end{aligned}$$

where the electric field is expressed in MV/m and power in MW. The beam power can be inferred from the spectrum measurement, with account taken of losses in the transport line. Following this procedure, one can obtain an experimental relationship between the position of the momentum peak and the gradient. For "low-current" running (i.e., running with less than 100 mA average current), we obtain reasonable agreement with simulations, as shown in Fig. 8.

High-current (i.e., greater than 100 mA average current) experimental data seem to indicate that the actual power going into electrons is about twice what can be accounted for based on measurements of beam power transmitted through the alpha magnet, possible explanations under investigation are secondary electrons generated in the gun,¹³ calibration errors in the detector diodes, stray external magnetic fields, and transverse RF fields due to coupling slots.

One can also compare measured momentum distributions to calculated momentum distributions by matching the peaks of the distributions. Because of the space-charge effect mentioned just above, this is subject to the ambiguity of not knowing the current density. However, this effect does not become prominent except at current densities in excess of about 30 A/cm². Since such current densities correspond to average currents in excess of 1 A, we do not expect to see significant broadening in the momentum spectrum for running below this current level. This expectation is confirmed by experiment, and an example of a comparison between a measured and simulated spectrum is shown in Fig. 9.

Simulations with MASK and *elegant* predict that it is possible to obtain bunch lengths of 1 ps for a wide variety of gun operating conditions. For our nominal operating gradient of 75 MV/m, a current density of 10 A/cm² is predicted to result in a peak-current of 125 A, with 6×10^9 electrons per S-band bunch and $\bar{\tau} = 22 \pi \cdot m_e c \cdot \mu\text{m}$. If the current density is increased to 40 A/cm², this becomes 347 A, with 2.3×10^9 electrons per bunch and normalized emittance of $\bar{\tau} = 23 \pi \cdot m_e c \cdot \mu\text{m}$.

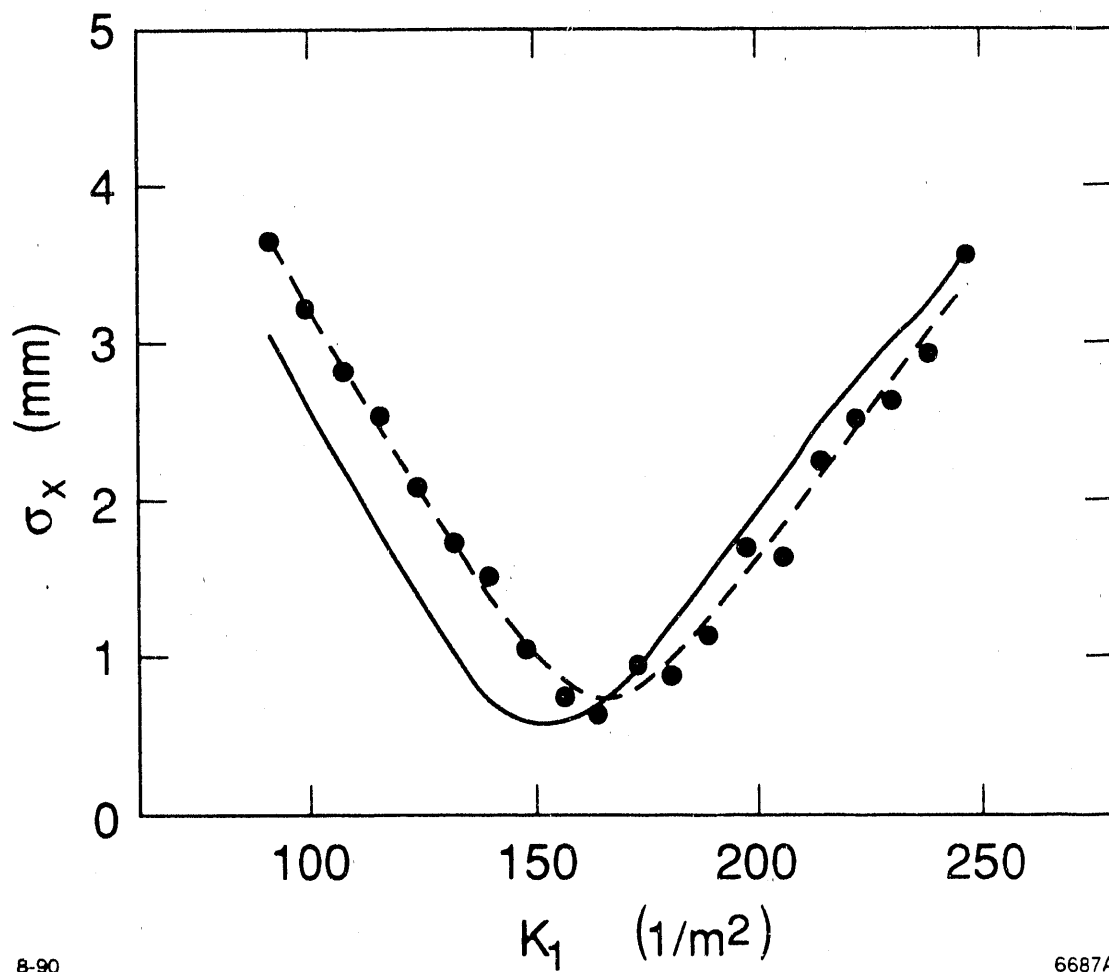
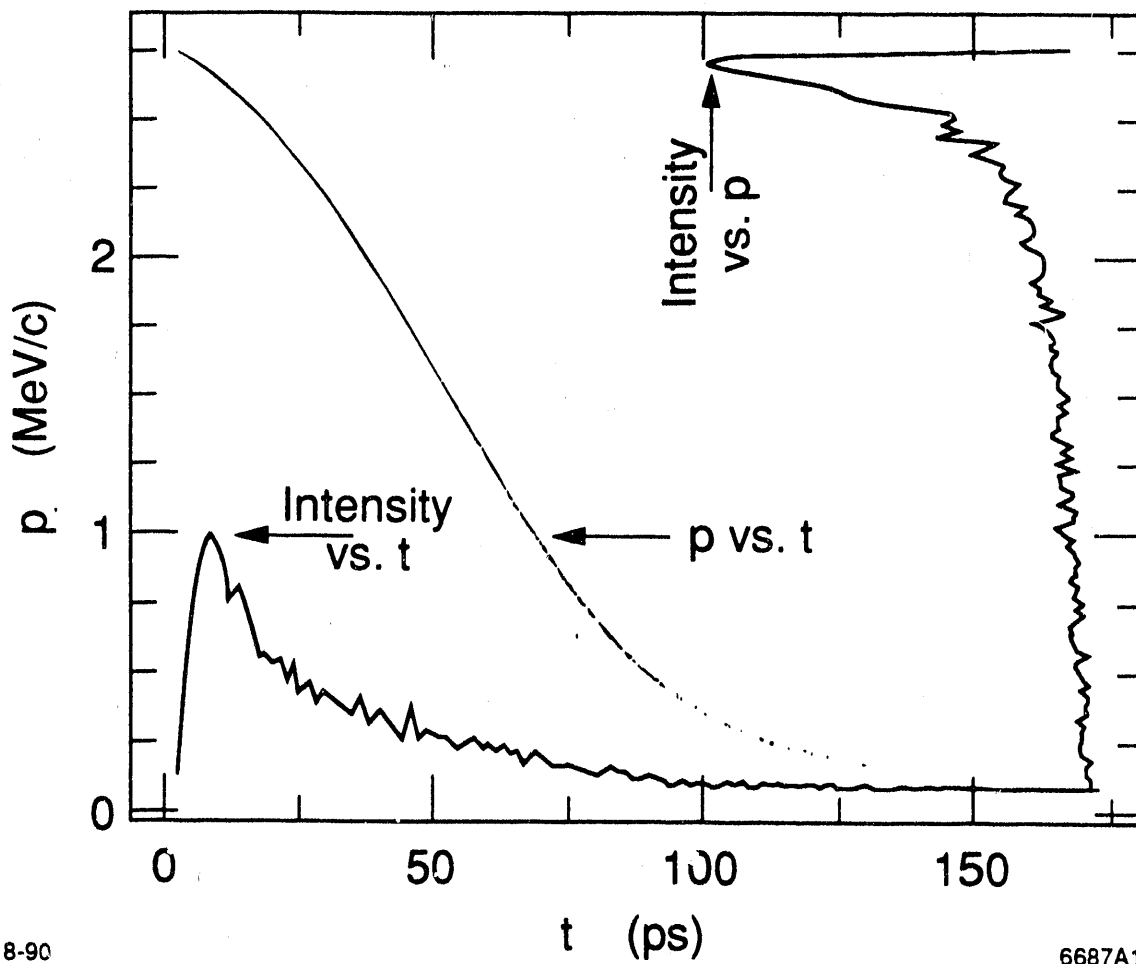


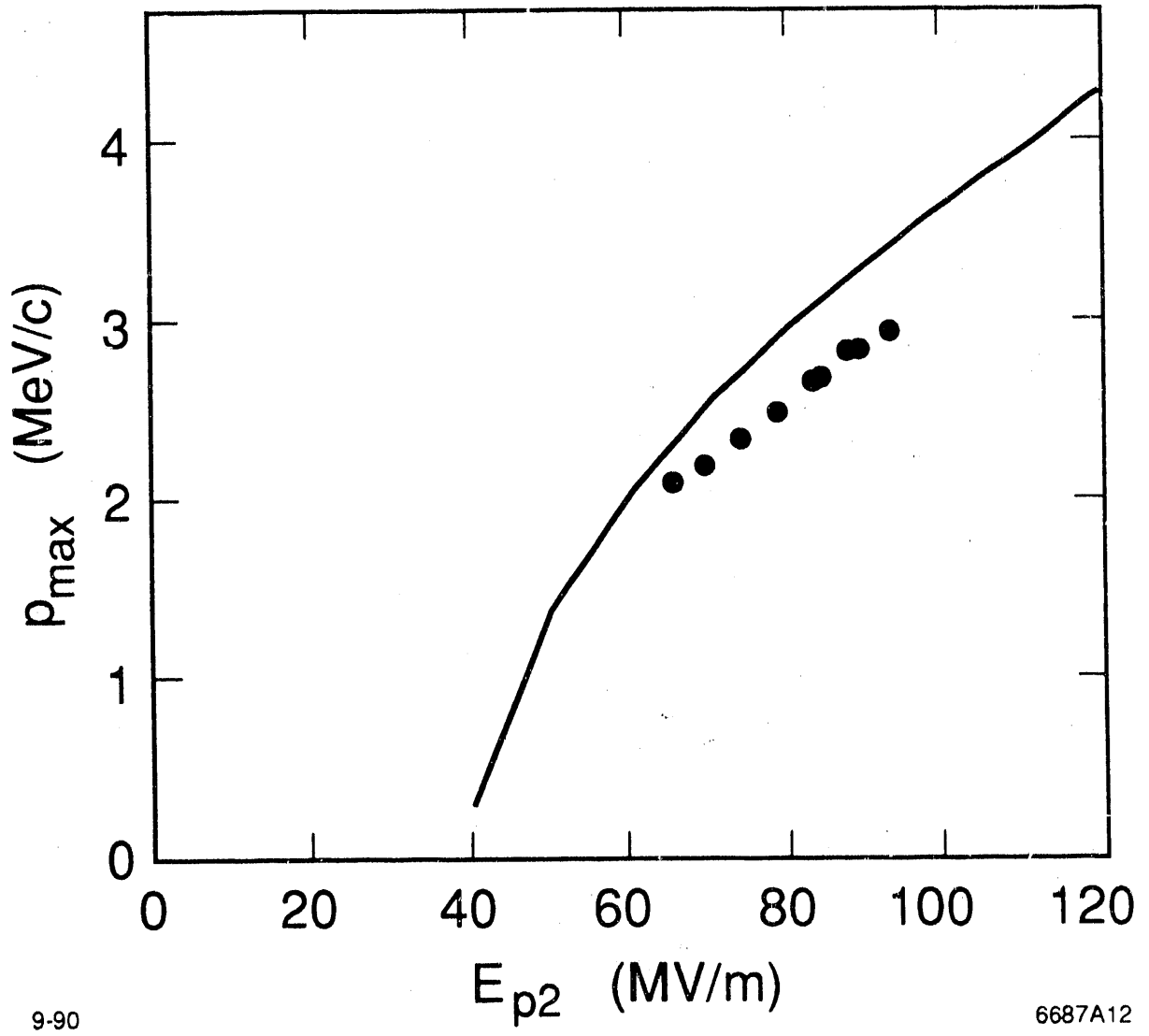
Fig. 6. Measured (points) and simulated (line) horizontal beam size, σ_x , versus quadrupole (GTLQ4) strength parameter, K_1 for beam parameters: $p = 2.7$ MeV/c, $\Delta p/p = \pm 10\%$ and $\dot{I} = 100$ mA. The normalized rms emittances then are 39 mm · mrad (measured) and 26 mm · mrad (simulated).



8-90

6687A14

Fig. 7. Gun longitudinal phase-space.



9-90

6687A12

Fig. 8. Maximum momentum versus peak electric field.

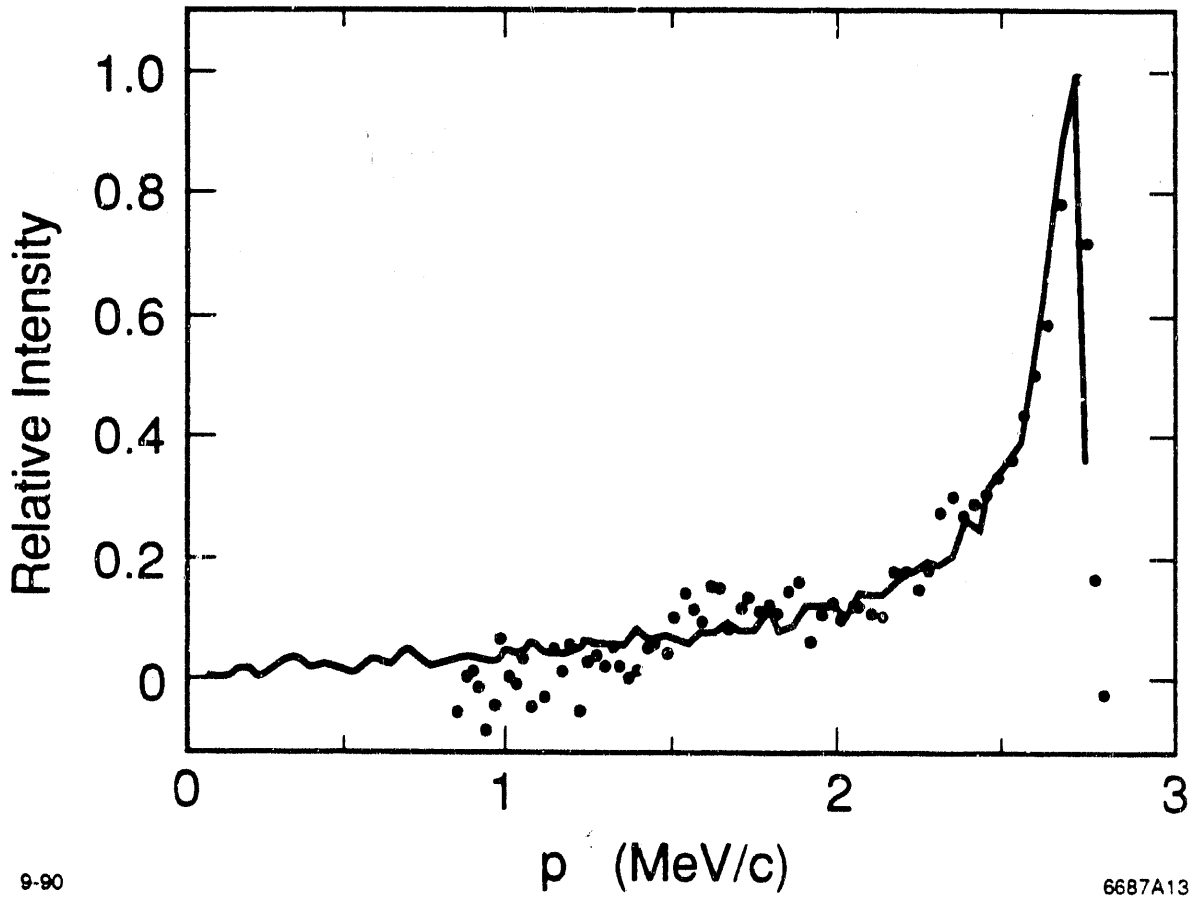


Fig. 9. Measured and simulated momentum spectra.

While this latter operating condition requires more RF power than available for the gun, the former operating condition has been achieved and exceeded, though the bunch length (and hence the peak current) has not been measured. Forthcoming experiments will attempt to measure the bunch length by using the third accelerator section phased at the field null, so as to introduce a time-dependent energy variation, which will be observed with a phosphorescent screen after a bending magnet. By measuring the dependence of energy spread on the field level in the third section, it should be possible to measure subpicosecond bunch lengths and hence test these predictions.

Acknowledgments

The authors wish to acknowledge the following people for contributions to design and engineering aspects of the gun project: M. Baltay, B. Youngman (SSRL), and R. McIntyre (Varian Associates). In addition, the following individuals provided technical and experimental support: C. Chavis, L. Emery, P. Colceff, J. Haydon, R. Hettel, B. Lavender, H. Morales, D. Mostowfi, J. Safranek, J. Sebek, D. Wang, C. Wermelskirchen (SSRL), W. Leong, S. Skellenger, and R. Tol (Varian Associates).

References

1. E. Tanabe *et al.*, "A 2 MeV Microwave Thermionic Gun," SLAC-PUB-5054 (1989).
2. T. I. Smith, "Intense Low-Emittance Linac Beams for Free-Electron Lasers," Proc. 1986 Linear Accelerator Conf., pp. 421-426.
3. G. A. Loew, R. H. Miller, C. K. Sinclair, "The SLAC Low-Emittance Accelerator Test Facility," Proc. 1986 Linear Accelerator Conf., pp. 144-147.
4. J. S. Fraser, "Electron Linac Injector Developments," Proc. 1986 Linear Accelerator Conf., pp. 411-415.
5. G. A. Westenskow, J. M. J. Madey, *Laser and Particle Beams*, Vol. 2, Pt. 2, 223-5 (1984).
6. R. L. Sheffield, E. R. Gray, J. S. Fraser, "The Los Alamos Photoinjector Program," *Nucl. Instrum. Methods*, 222-226 (1988).
7. K. T. McDonald, "Design of the Laser-Driven RF Electron Gun for the BNL Accelerator Test Facility," *IEEE J. of Quantum Electron* **QE-23**, 1489-96 (1987).
8. A. T. Drzobot *et al.*, "Numerical Simulation of High Power Microwave Sources," *IEEE Trans. NS-32*, 2733-7 (1985).
9. M. Borland, Ph.D. thesis, Stanford University, to be published.
10. H. A. Enge, "Achromatic Magnetic Mirror for Ion Beams," *Rev. Sci. Instrum.* **34**, No. 4, 385-389 (1963).
11. K. L. Brown, "A First- and Second Order Matrix Theory for the Design of Beam Transport Systems and Charged Particle Spectrometers," SLAC Report-75 (1982).
12. See, e.g., M. C. Ross *et al.*, "Automated Emittance Measurements in the SLC," SLAC-PUB-4278 (1987).
13. R. L. Sheffield, private communication.

DISCLAIMER

This report was prepared as an account of work sponsored by an agency of the United States Government. Neither the United States Government nor any agency thereof, nor any of their employees, makes any warranty, express or implied, or assumes any legal liability or responsibility for the accuracy, completeness, or usefulness of any information, apparatus, product, or process disclosed, or represents that its use would not infringe privately owned rights. Reference herein to any specific commercial product, process, or service by trade name, trademark, manufacturer, or otherwise does not necessarily constitute or imply its endorsement, recommendation, or favoring by the United States Government or any agency thereof. The views and opinions of authors expressed herein do not necessarily state or reflect those of the United States Government or any agency thereof.

END

DATE FILMED

12 / 26 / 90

